Brain Stimulation 8 (2015) 758–768

Contents lists available at ScienceDirect

Brain Stimulation

journal homepage: www.brainstimjrnl.com

Subcallosal Cingulate Connectivity in Anorexia Nervosa Patients Differs From Healthy Controls: A Multi-tensor Tractography Study

Dave J. Hayes [a,b,c], Nir Lipsman [a,b,c], David Q. Chen [a,b,c], D. Blake Woodside [d], Karen D. Davis [a,b,c], Andres M. Lozano [a,b,c], Mojgan Hodaie [a,b,c,*]

[a] Institute of Medical Science, University of Toronto, Toronto, Ontario, Canada
[b] Toronto Western Research Institute, Division of Brain, Imaging and Behaviour – Systems Neuroscience, University Health Network, Toronto, Ontario M5T 2S8, Canada
[c] Division of Neurosurgery, Department of Surgery, Toronto Western Hospital, 399 Bathurst Street, Toronto, Ontario M5T 2S8, Canada
[d] Department of Psychiatry, University of Toronto, Toronto General Hospital, 200 Elizabeth Street, Toronto, Ontario M5G 2C4, Canada

ARTICLE INFO

Article history:
Received 18 November 2014
Received in revised form
18 March 2015
Accepted 21 March 2015
Available online 12 June 2015

Keywords:
Diffusion tensor imaging
DTI
Eating disorder
Mood disorder
Fractional anisotropy
Deep brain stimulation

ABSTRACT

Background: Anorexia nervosa is characterized by extreme low body weight and alterations in affective processing. The subcallosal cingulate regulates affect through wide-spread white matter connections and is implicated in the pathophysiology of anorexia nervosa.
Objectives: We examined whether those with treatment refractory anorexia nervosa undergoing deep brain stimulation (DBS) of the subcallosal white matter (SCC) show: 1) altered anatomical SCC connectivity compared to healthy controls, 2) white matter microstructural changes, and 3) microstructural changes associated with clinically-measured affect.
Methods: Diffusion magnetic resonance imaging (dMRI) and deterministic multi-tensor tractography were used to compare anatomical connectivity and microstructure in SCC-associated white matter tracts. Eight women with treatment-refractory anorexia nervosa were compared to 8 age- and sex-matched healthy controls. Anorexia nervosa patients also completed affect-related clinical assessments presurgically and 12 months post-surgery.
Results: 1) Higher (e.g. left parieto-occipital cortices) and lower (e.g. thalamus) connectivity in those with anorexia nervosa compared to controls. 2) Decreases in fractional anisotropy, and alterations in axial and radial diffusivities, in the left fornix crus, anterior limb of the internal capsule (ALIC), right anterior cingulum and left inferior fronto-occipital fasciculus. 3) Correlations between dMRI metrics and clinical assessments, such as low pre-surgical left fornix and right ALIC fractional anisotropy being related to post-DBS improvements in quality-of-life and depressive symptoms, respectively.
Conclusions: We identified widely-distributed differences in SCC connectivity in anorexia nervosa patients consistent with heterogenous clinical disruptions, although these results should be considered with caution given the low number of subjects. Future studies should further explore the use of affect-related connectivity and behavioral assessments to assist with DBS target selection and treatment outcome.

Abbreviations: AD, axial diffusivity; ALIC, anterior limb of the internal capsule; BAI, Beck Anxiety Inventory; BDI, Beck Depression Inventory; Cing, cingulum; CC, corpus callosum; dMRI, diffusion magnetic resonance imaging; FA, fractional anisotropy; HAMD, Hamilton Depression Inventory; IFO, inferior fronto-occipital fasciculus; MTT, multi-tensor tractography; PTR, posterior thalamic radiation; QOL, quality-of-life scale; RD, radial diffusivity; ROI, region-of-interest; SCC, subcallosal cingulate white matter; YBC (P, R), Yale-Brown-Cornell Eating Disorder Scale (Preoccupations and Ritualistic subscales); YBOCS, Yale-Brown Obsessive Compulsive Scale.

This work was made possible by grants from the Klarman Family Foundation Grants Program in Eating Disorders Research (AML) and a Canadian Institutes of Health Research Operating Grant (MH). NL holds a Fellowship from the Canadian Institutes of Health Research (CIHR 130555). AML is a Tier 1 Canada Research Chair in Neuroscience. Funding agencies had no role whatsoever in design and conduct of the study, collection, management, analysis, and interpretation of the data, or preparation, review, or approval of the manuscript, or the decision to submit the manuscript for publication.

Conflicts of interest: DJH, NL, DQC, DBW, KD and MH declare that they have no biomedical financial interests or potential conflicts of interest. AML is a consultant for St Jude Medical, Medtronic and Boston Scientific, and holds intellectual property related to brain stimulation for depression.

* Corresponding author. Division of Neurosurgery, Department of Surgery, University of Toronto, 399 Bathurst Street, Toronto, Ontario M5T 2S8, Canada. Tel.: +1 416 603 5800.
E-mail address: Mojgan.hodaie@uhn.ca (M. Hodaie).

http://dx.doi.org/10.1016/j.brs.2015.03.005

Anorexia nervosa is a challenging and heterogenous disorder with the highest mortality rate of any psychiatric disease [1,2]. Characterized by a relentless pursuit of thinness and distorted body perceptions, anorexia nervosa's psychological impairments and psychiatric comorbidities pose the greatest treatment challenge. Although some treatments are available, few psycho- and pharmacotherapeutic options are effective and enduring [3,4]. As a result, an estimated one-third to a half of anorexia nervosa patients are refractory to currently available treatments, resulting in high rates of relapse, illness chronicity, and risk of mortality [5].

Brain imaging has contributed significantly to our understanding of the neural correlates of the cardinal features of anorexia nervosa, including affective disturbances. Studies have identified a network of key regions linked to affective processing that function differently in anorexia nervosa compared to healthy people [6]. For example, those with anorexia nervosa have lower baseline activity in the bilateral parietal and prefrontal cortices, specifically in anterior cingulate and subcallosal cingulate cortices [7,8]. Anterior cingulate activity also increases in response to food-related stimuli in anorexia nervosa relative to controls [9,10]. Other studies have shown that the dysregulated anorexia nervosa network also includes the thalamus, insula, amygdala, hippocampus, and striatum [7,8,11–14]. These results underscore the importance of affective brain processing in the symptomology of anorexia nervosa, and suggest that affective regulation and disturbances play a key role in the maintenance of symptoms [6].

Our group has investigated the use of deep brain stimulation (DBS) in patients with chronic, treatment-resistant, anorexia nervosa [15]. Subcallosal cingulate white matter (SCC) was chosen as the DBS target given its role in affective regulation as well as anatomic and physiologic links to important emotion and reward processing [15–18], as well as abnormal serotonin receptor binding in people with eating disorders [19,20]. Furthermore, the SCC is a widely-connected hub that contains appetitive- and aversive-responsive cells projecting to anorexia nervosa-affected regions, such as areas of the prefrontal, parietal and temporal cortices, insula, striatum and amygdala [6,21–23]. Despite these findings, little is known about the structural white matter abnormalities in anorexia nervosa related to such functional and clinical abnormalities.

The present study used deterministic multi-tensor tractography (MTT) and a region-of-interest (ROI) approach to investigate the hypotheses that: 1) the SCC has differential connectivity in those with anorexia nervosa compared to healthy controls; 2) areas along the identified white matter tracts have altered diffusion magnetic resonance imaging (dMRI) metrics, such as changes in fractional anisotropy (FA), axial (AD) and radial (RD) diffusivity and 3) these abnormalities correlate to clinically-measured affective dysfunction in anorexia nervosa. We chose the MTT approach over others because multiple tensors improve the detection of fibers that are dense, highly crossing or angled, and/or travel over long distances [24–26]. Although considered cautiously in light of a low sample size, our findings help identify broad underlying changes in white matter microstructure associated with the heterogenous clinical profile of anorexia nervosa.

Material and methods

Participants

This study included eight female patients with treatment-refractory anorexia nervosa (mean age: 35 ± 11 years), age-matched to eight female healthy controls (CN; 36 ± 9 years). Participants were identified by centers within the University Health Network (Toronto, Canada). Patients were referred through the eating disorders programme at Toronto General Hospital, and healthy participants recruited from advertisements in the Toronto Western Hospital. Selected patients underwent implantation of bilateral electrodes in the SCC. Ethics approval was granted by the University Health Network Research Ethics Board and all subjects gave their informed written consent. Inclusion and exclusion criteria have been detailed elsewhere [15] and can be found in Supplementary Methods. Patient demographic information is in Table 1.

Magnetic resonance acquisition and preprocessing of diffusion weighted images

MR images were acquired using an 8-channel phased-array head coil on a GE Signa HD×t 3T scanner (GE Healthcare, WI, USA). Diffusion-weighted images were acquired using 60 non-collinear directions over a 12 min period with a dual-spin echo planar sequence, to reduce eddy-current distortions, using the Array Spatial Sensitivity Encoding Technique (ASSET) factor of 2 and the following parameters: 0.94 × 0.94 × 3.0 mm voxels, 128 × 128 matrix, FOV = 24 cm, TE = 86.4 ms, TR = 12 s, b = 1000 s/mm^2. Anatomical T1-weighted axial images were acquired with a 3D Fast Spoiled Gradient Echo sequence (see full parameters in Supplementary Methods).

Scans underwent preprocessing and registration using the FSL v 5.0 (FMRIB Software Library, http://fmrib.ox.ac.uk/fsl) [27] and 3D Slicer v 4.3.1 (NA-MIC©, http://www.slicer.org) [28] suite of brain imaging analysis tools in a Linux environment. Diffusion-weighted scans were motion- and eddy-current corrected in FSL and imported to 3D Slicer for T1 to diffusion-weighted baseline linear registration and visualization, tensor estimation and the creation of scalar maps for fractional anisotropy (FA), axial diffusivity (AD), and radial diffusivity (RD) at the individual level.

Table 1
AN patient demographic data.

Patient number	Age at surgery	Age at Onset	Duration of illness	Lowest lifetime BMI	Highest lifetime BMI	Comorbidities	Medications
A01	24	14	10	9.6	47.3	AN, MDD, Anxiety	Zoloft, Seroquel, Cytomel, Lactulose, Colace, Co Pantoprozole
A02	39	18	21	12.3	21	AN-BP, MDD, PTSD, OCD	Imovane, Clonazepam, Quetiapine, Pantoloc, Domperidone, Sertraline, Lactulose, Colace, K-Dur, Tobramycin, Acetaminophin, Advil Cold & Sinus, Laxatives
A03	35	20	15	13.3	23.3	AN, MDD, PTSD	Celexa
A04	40	30	10	13.3	30	AN, MDD, PTSD	Quetiapine, Fluoxetine, Pantoloc, Domperidone maleate, Docusate sodium, Nabilone, Diclofenac sodium, Lithium carbonate, Lactulose
A05	35	16	19	13.3	21.3	AN-BP, MDD, PTSD, GAD	Fluoxetine, Gabapentin, Quetiapine, Acetaminophen, Docusate, Indian psyllium husks, Calcium, Vitamin D
A06	57	30	27	13.7	19.4	AN	Iron, Calcium, Vitamin D
A07	21	12	9	11.2	20.6	AN-R, MDD, GAD, OCD traits, BPD	Quetiapine, Trazodone, Venlafaxine, Maalox, Ibrupofen, Lactulose, Lactaid
A08	32	13	19	12.9	21.5	AN-BP, MDD, PTSD	Venlafaxine, Seroquel, Trazodone, Zopiclone, Docusate Sodium, Lactulose

As recommended by others [29], we corrected the *b*-matrices with finite strain correction by averaging the rotational component of the gradient affine transforms and then applied these to the original *b*-matrices.

Multi-tensor tractography (MTT) using subcallosal cingulate (SCC) region-of-interest (ROI)

The eXtended Streamline Tractography, or XST, algorithm was used for whole-brain deterministic multi-tensor tractography (MTT) implemented in 3D Slicer software [26]. The deterministic MTT approach was chosen over others to improve the detection of fibers that are dense, crossing, highly angled, and/or travel over long distances [24–26]. Moreover, we were interested in whole-brain connectivity to the SCC region and Khalsa et al. (2013) recently showed that probabilistic tractography is inferior to deterministic MTT in reconstructing longer pathways. MTT maps were generated using a ROI that included the middle two of a four-contact electrode and contained the active contact (model 3387, Medtronic, Minneapolis, MN, USA). The patients' co-registered post-surgical T1 image was used to draw bilateral SCC ROIs (located in the white matter below the genu of the corpus callosum) in pre-surgical FA map space. This was achieved by co-registering the post-surgical T1 image to the already FA-transformed pre-surgical T1 image. SCC ROIs in healthy subjects were anatomically matched to the patient's (see Fig. 1, left panel). Bilateral whole-tract and SCC ROI measures of FA, AD, and RD were compared statistically by Analysis of Variance (ANOVA), performed in SPSS 17.0 statistical software (SPSS, Chicago, IL, USA). Individual MTT models (see Fig. 1, right panel) from patient and healthy groups were combined, to create binarised and non-binarised group maps, similar to that noted in a previous study of major depressive disorder [30]. See Supplementary Methods for additional parameters.

ROI analysis along MTT maps

ROIs were selected based on MTT group map connectivity patterns (Fig. 2A). Chosen ROIs were in areas showing indices of higher, lower, and similar connectivity strength in anorexia nervosa subjects compared to controls, on at least one side of the brain (Fig. 2B). The following three groups of ROIs were selected: 1) increased connectivity ROIs (anorexia nervosa greater than control subjects: AN $>$ CN) in the fornix crus, junction of the posterior thalamic radiation/superior longitudinal fasciculus (PTR/SLF), and corpus callosum splenium (CC Splen); 2) decreased connectivity ROIs (AN $<$ CN) in the anterior limb of the internal capsule (ALIC), anterior cingulum (Ant Cing), and inferior fronto-occipital fasciculus (IFO); 3) two control ROIs located in regions with apparent overlapping connectivity (AN $\cap$ CN) in the posterior cingulum (Post Cing) and corpus callosum genu (CC Genu). A single CC Genu ROI was selected along the midline, given the absence of asymmetry in the MTT maps. dMRI metrics (i.e. FA, AD, RD) were extracted from each ROI, and repeated measures ANOVAs (side $\times$ dMRI metric), with group as a between-group measure, followed by appropriate post-hoc tests, were performed. Briefly, 8 repeated measures ANOVAs (side $\times$ dMRI metric), with group as a between-group measure, were used for each ROI to test within- and between-group differences. Main (side $\times$ dMRI metric $\times$ group; SDG) and subordinate interaction terms were considered (i.e. side $\times$ dMRI, SD; side $\times$ group, SG; dMRI $\times$ group, DG). Significant interaction results were followed with appropriate post-hoc *t*-tests, and paired-samples *t*-tests were used to investigate within-subject side differences.

Clinical assessment and exploratory dMRI-clinical correlation analysis

Patients underwent psychometric assessments at baseline, prior to surgery, and post-surgery at 1, 3, 6, and 12 months (only scores at

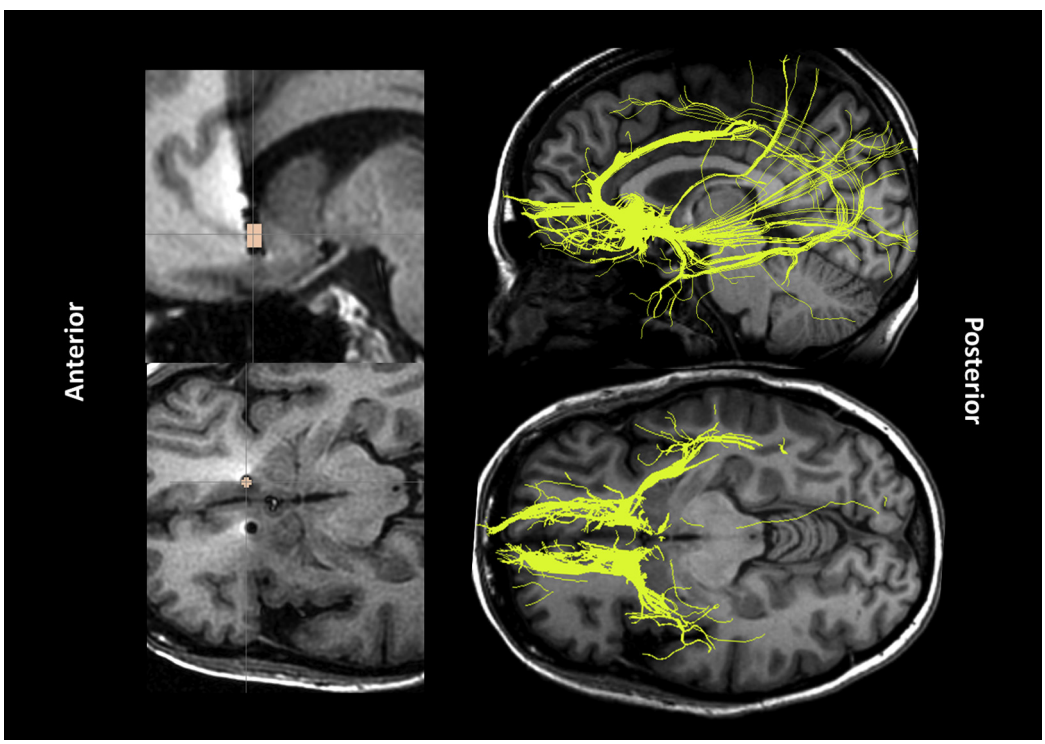

Figure 1. Placement of SCC electrode/seed and individual MTT map. **Left panel:** Sample SCC seed placement. Individual T1 anatomical images following surgery were used to locate the site of the electrode (MNI coordinates: ±12, 24, -10) and to place the SCC seed in dMRI space (always in a cross-shaped pattern at the mid-electrode level using 24 voxels, with a volume of 63 mm^3). **Right panel:** Sample individual multi-tensor tractography map for one subject with anorexia nervosa.

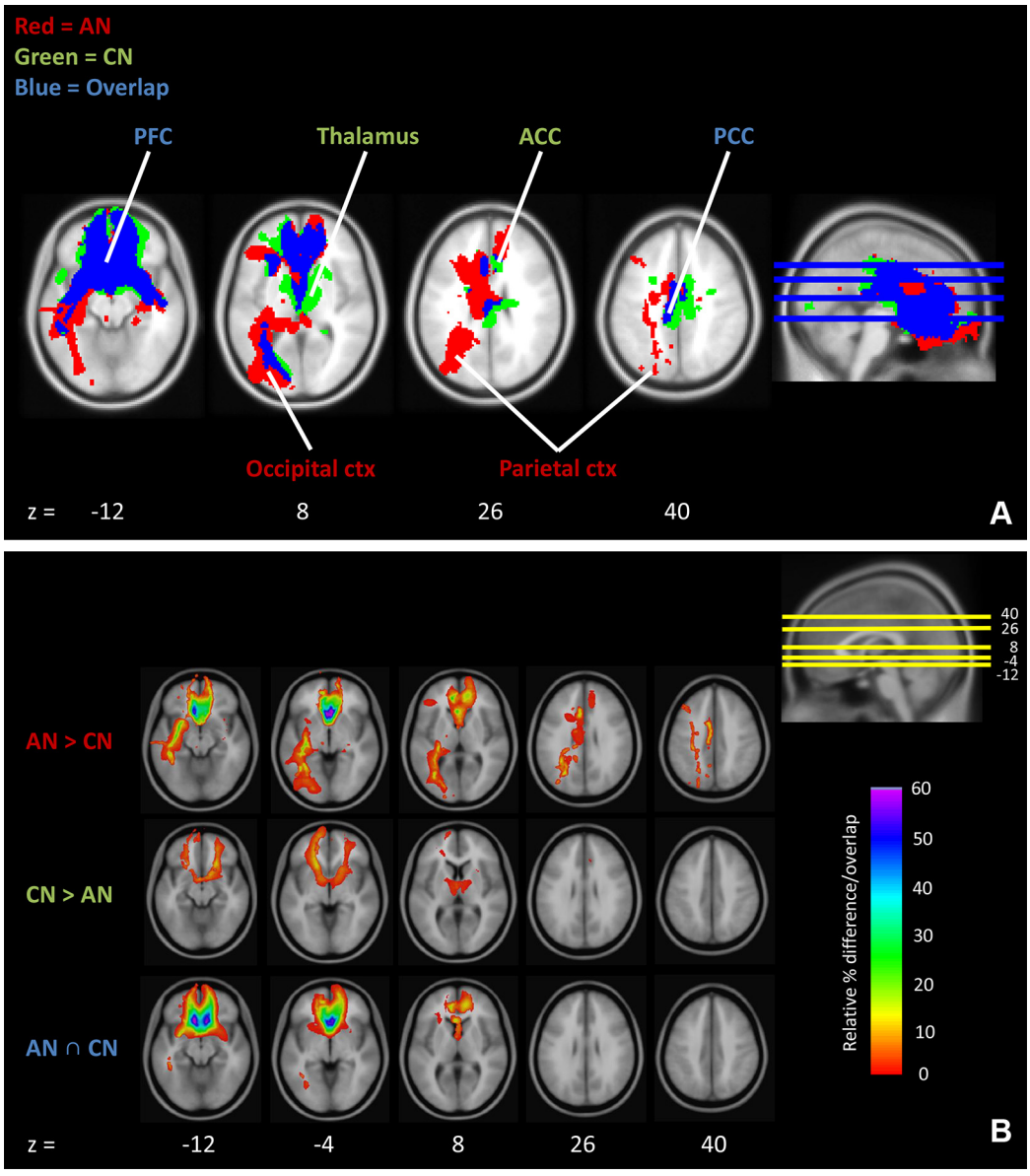

Figure 2. A: Group MTT connectivity pattern maps in AN and healthy controls. B: Group MTT connectivity strength maps in AN and healthy controls. **A:** Connectivity pattern multi-tensor tractography maps at the group level reveals connectivity which appears unique to anorexia nervosa (AN > CN; red) or healthy controls (CN > AN; green), implying an increase and decrease in SCC connectivity in anorexia nervosa, respectively, relative to controls. Apparently overlapping connectivity (AN ∩ CN; blue) between groups is also noted - though given the spatial limitations of such data, it is important to note that this overlap does not necessarily imply similar connectivity. These maps are a spatial illustration of apparent connectivity from the SCC seed at the group level, following the smoothing (1mm kernel), binarisation, and MNI space registration of individual deterministic MTT maps. **B:** Connectivity strength group MTT maps emphasise findings from the connectivity pattern data, but also suggest increased connectivity to the medial prefrontal and left parieto-occipital cortices in anorexia nervosa, and lower connectivity in thalamus. These results are supported further at the individual level (see Table 2). The color bar reflects the relative % difference or overlap (i.e. relative strength of connectivity) of voxels based on the subtraction (i.e. AN > CN; CN > AN) or addition (AN ∩ CN) of smoothed, non-binarised, and MNI space registered group tract models (see Materials and Methods for details).

12 months and percent changes, from 0 to 12 months, are considered here). Assessments included: HAMD [31], BDI [32], BAI [33], YBOCS [34], YBC-EDS (including subscales for ritualistic behaviors and preoccupations related to food) [35] and QOL [36]. Given the *a priori* hypothesis that structural differences in white matter may be related to the affective disruptions noted in anorexia nervosa [6], we correlated significant findings in ROI dMRI metrics with clinical scores, using Pearson partial correlation analysis with brain volume and BMI at the time of surgery as regressors-of-no-interest. Individual brain volumes were estimated in 3D Slicer as the combined volume of gray and white matter masks. Given the exploratory nature of such correlations, due to our low sample size, we did not correct for multiple comparisons.

Results

Multi-tensor tractography (MTT) maps show differential patterns of connectivity in anorexia nervosa vs. control subjects

Deterministic MTT group maps identified differential structural connectivity patterns and strengths from the SCC seed region in healthy controls (CN) and patients with anorexia nervosa (Fig. 2). Connectivity to common regions, identified by the conjunction of each map (AN ∩ CN), included: prefrontal (PFC), bilateral temporal, left mid and posterior cingulate, and occipital cortices, and ventral striatum (Fig. 2A). Anorexia nervosa-selective regions (AN > CN) included: left occipital, parietal and dorsolateral prefrontal cortices,

and left cerebellum. Anorexia nervosa-selective extensions also noted were: bilateral orbitofrontal, right dorsomedial prefrontal and left cingulate cortices (lateral to area noted above). Regions noted in the healthy control group (CN > AN) included: thalamus, mid and anterior cingulate, and left anterior temporal cortices, with extensions in bilateral ventrolateral PFC, left medial occipital, right anterior insular and midcingulate cortices.

Non-binarised MTT maps (Fig. 2B) suggested that connectivity within the medial PFC and left parieto-occipital cortex may be stronger, and thalamic connectivity weaker, in anorexia nervosa subjects. Visual inspection of the MTT maps at the individual level further emphasized these differences (Table 2). Moreover, parietal cortex connectivity was predominantly ipsilateral, while thalamic connectivity in controls appears bilateral.

A repeated measures ANOVA revealed no significant interactions across groups or brain sides for SCC ROI dMRI metrics (side × dMRI metric × group: $F_{3,39} = 0.001$, $P = 1.0$; dMRI × side: $F_{3,39} = 0.04$, $P = 0.99$; dMRI × group: $F_{3,39} = 0.76$, $P = 0.52$; side × group: $F_{3,39} = 0.003$, $P = 0.96$). However, a significant interaction from dMRI data extracted and averaged along the entire MTT pathways was noted (side × dMRI metric × group: $F_{3,39} = 8.65$, $P < 0.001$). Post-hoc paired *t*-tests revealed that while right side whole-tract FA (0.344) was lower than the left (0.368) within-anorexia nervosa subjects ($P = 0.015$), it was not significantly different ($P = 0.087$) from the mean right FA in healthy subjects (FA = 0.366).

ROI analysis along MTT maps suggests regionally-selective differences between groups

Selected ROIs are illustrated in Fig. 3A and associated dMRI findings are summarized in Fig. 3B–D. The pattern of results (i.e. changes in FA, AD, RD) was unique to each brain region. The following are the interaction results of the repeated measures ANOVAs (by side × dMRI metrics × group; SDG) across the 8 ROIs, with significant interactions in bold: **ALIC** – SDG ($F_{4,52} = 1.87$, $P = 0.13$), SD ($F_{4,52} = 0.77$, $P = 0.55$), **DG ($F_{4,52} = 16.44$, $P < 0.001$)**, SG ($F_{4,52} = 1.87$, $P = 0.19$); **Ant Cing** – SDG ($F_{4,52} = 0.62$, $P = 0.65$), SD ($F_{4,52} = 0.34$, $P = 0.85$), **DG ($F_{4,52} = 6.62$, $P < 0.001$),** SG ($F_{4,52} = 0.63$, $P = 0.44$); **CC Genu** – DG ($F_{4,52} = 0.54$, $P = 0.70$); **CC Splen** – SDG ($F_{4,52} = 2.04$, $P = 0.10$), SD ($F_{4,52} = 0.40$, $P = 0.81$), DG ($F_{4,52} = 0.04$, $P = 0.99$), SG ($F_{4,52} = 2.03$, $P = 0.18$); **Fornix crus – SDG ($F_{4,52} = 7.55$, $P < 0.0001$),** SD ($F_{4,52} = 0.41$, $P = 0.80$), DG ($F_{4,52} = 0.36$, $P = 0.84$), **SG ($F_{4,52} = 7.51$, $P = 0.017$); IFO** – SDG ($F_{4,52} = 2.00$, $P = 0.11$), SD ($F_{4,52} = 0.88$, $P = 0.48$), **DG ($F_{4,52} = 7.33$, $P < 0.001$),** SG ($F_{4,52} = 2.00$, $P = 0.18$); **Post Cing** – SDG ($F_{4,52} = 0.66$, $P = 0.62$), SD ($F_{4,52} = 0.12$, $P = 0.94$), DG ($F_{4,52} = 0.03$, $P = 0.99$), SG ($F_{4,52} = 0.66$, $P = 0.43$); **PTR** – SDG ($F_{4,52} = 2.38$, $P = 0.063$), SD ($F_{4,52} = 0.04$, $P = 0.99$), DG ($F_{4,52} = 0.91$, $P = 0.46$), SG ($F_{4,52} = 2.36$, $P = 0.15$).

In brief, only the fornix crus was found significant for the side × dMRI metric × group interaction ($F_{4,52} = 7.55$, $P < 0.001$), while the PTR/SLF showed 'trend-level' significance ($F_{4,52} = 2.38$, $P < 0.06$). Post-hoc analysis ($P < 0.05$) revealed that only the left fornix crus showed a lower FA in patients compared to controls which was accompanied by an increase in RD and no change in AD. Among lower connectivity ROIs, all regions showed a significant interaction of dMRI metric × group (ALIC: $F_{4,52} = 16.44$, $P < 0.001$; Ant Cing: $F_{4,52} = 6.62$, $P < 0.001$; IFO: $F_{4,52} = 7.33$, $P < 0.001$). FA values were lower compared to controls for the bilateral ALIC and left IFO, and were accompanied by bilateral increases in ALIC and IFO RD values. Right ALIC and Ant Cing showed decreased AD values compared to controls.

Clinical assessment and exploratory dMRI-clinical correlation analysis

All clinical measures were selectively correlated to ROIs previously shown to differ between control and anorexia nervosa subjects (Table 3). Briefly, post-surgical clinical measures of affect correlated with left fornix FA and RD, right ALIC FA, AD, and RD, right Ant Cing AD, left IFO FA and RD, and right IFO RD. Selected partial correlations are illustrated in Fig. 4. For illustrative purposes, individual clinical improvements from pre- to post-surgery are noted in Table 4.

Discussion

This study identified differential connectivity from the subcallosal cingulate white matter (SCC) in treatment-refractory patients with anorexia nervosa compared to controls. Connectivity measures in anorexia nervosa, identified by deterministic multitensor tractography (MTT) (Fig. 2, Table 2), suggest higher connectivity in the prefrontal and left parieto-occipital cortices, and lower connectivity in the thalamus. Decreases in fractional anisotropy (FA; a metric of water diffusivity along tracts), and corresponding AD decreases and RD increases, were seen within the anterior limb of the internal capsule (ALIC), left fornix crus and inferior fronto-occipital fasciculus (IFO), and right anterior cingulum (Ant Cing) (Fig. 3). However, the SCC itself did not show differences in dMRI metrics within or between groups. Although this might suggest that the symptoms of anorexia nervosa are not related to white matter

Table 2
Visual inspection of individual MTT maps.

	Ipsilateral				Contralateral				Total		# of subjects with connection from either ROI to brain area on either side	
	L AN	L CN	R AN	R CN	L AN	L CN	R AN	R CN	AN	CN	AN	CN
vmPFC	8	8	8	8	7	4	8	6	31	26	8	8
dmPFC	6	4	7	6	3	1	2	2	18	13	7	8
Parietal	6	1	5	1	1	1	2	2	14	5	8	3
Occipital	4	1	1	2	1	1	0	2	6	6	5	3
Temporal	6	3	6	4	2	1	1	2	15	10	7	5
Insula	6	6	3	6	0	1	1	0	10	13	6	7
V. striatum	6	4	4	7	2	1	0	2	12	14	8	8
Thalamus	1	3	0	5	0	2	0	2	1	12	1	8

MTT maps were inspected for individual connectivity from SCC seed to other macroscopic areas. Connectivity from the left and right SCC seed regions was investigated separately, and ipsilateral and contralateral connections were counted and totalled.
Right column: The number of subjects showing connections from either SCC seed region to a brain region, either contra- or ipsi-laterally, was also summarized for illustrative purposes. Note that apparent discrepancies between this column and others are because many subjects had *both* ipsilateral and contralateral projections from the SCC ROI. For instance, 3 CN subjects showed bilateral SCC-occipital connectivity, while 6 similar connections noted in anorexia nervosa subjects were distributed across 5 people.

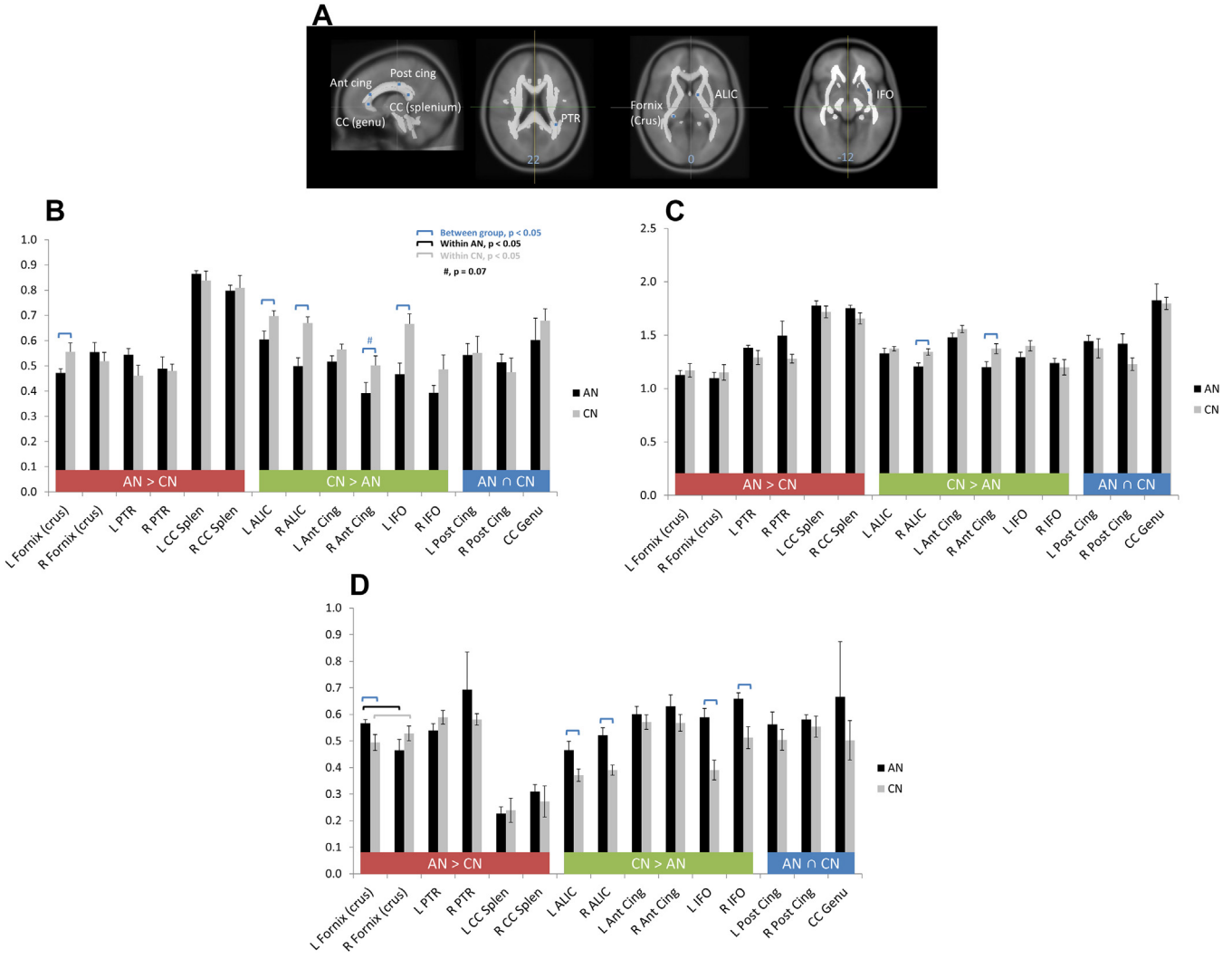

Figure 3. A: Regions-of-interest (ROI) placement along tracts. B: Mean FA values for ROIs along group MTT maps. C: Mean AD values for ROIs along group MTT maps. D: Mean RD values for ROIs along group MTT maps. **A:** ROIs were chosen based on findings noted in Figure 2. Regions were selected for their apparent increased (fornix crus, PTR, CC Splen), decreased (ALIC, Ant Cing, IFO), or similar (Post Cing, CC Genu) connectivity levels in anorexia nervosa compared to controls. ROIs (8 voxels/64 mm^3 each) were drawn in two adjacent axial slices (four voxels in each of two slices) on the MNI152 T1 anatomical template (representing the average of 152 healthy scans) along main white matter tracts, as identified by the DTI-81 atlas, and back-projected to individual space for dMRI metric extractions. Numbers represent the MNI z-coordinate. **B-D:** Mean ROI-based fractional anisotropy (FA), axial diffusivity (AD), and radial diffusivity (RD) values between anorexia nervosa (black) and control (beige) groups. Blue bars = group difference; black bars = within-anorexia nervosa-group difference; beige bars = within-CN-group difference; # is $p = 0.07$. Error bars are standard error of the mean.

deficits in the SCC region, this interpretation must be considered with caution given the relatively low-powered nature of the study. It is, for instance, possible that subtle but consistent changes in this region in patients with AN are not detectable at this level (i.e. $n = 8$) or even given the inherent signal-to-noise limitations in our dMRI acquisitions. Nonetheless, the finding of white matter alterations along a number of regions which appear connected to the SCC (i.e. ALIC, IFO, Ant Cing, left fornix crus) further supports the possibility that the SCC target is effective at least in part because of its connectivity to regions with disorder-related white matter alterations. Finally, an exploratory analysis found that FA values in left fornix and IFO, and right ALIC were correlated to changes in clinical affective measures related to eating behavior, quality of life, and anxiety as well as depressive symptoms, respectively (Table 3).

Together, these results support the continued development of connectivity profiles as individualized tools toward the improvement of psychiatric treatments — for instance, in improving target selection for those patients undergoing DBS. Moreover, these data have wider implications relating to the study of affect, emotion, and mood — as is underscored, for instance, by similar findings in major depressive disorder [21,37].

SCC connectivity is different between anorexia nervosa and controls subjects

The most prominent differences between anorexia nervosa and controls were increased connectivity to the ipsilateral parietal cortex and decreased connectivity to the thalamus bilaterally (Fig. 2, Table 2). These differences are not likely driven by noise in the data given that individual tract inspection revealed many equally connected regions in AN and CN groups (e.g. vmPFC, ventral striatum), as well as clear differences between the groups (e.g. parietal cortex, thalamus), and there is no reason to suspect systematic differences in signal-to-noise between these two groups (e.g. as acquisitions occurred at the same site/scanner). To our knowledge, this is the first report identifying such differences and these results are in line with known functional brain abnormalities in anorexia nervosa subjects [38,39].

Table 3
dMRI metrics and clinical affect-related measures.

		dMRI metrics		
Map-type	ROI	FA (Clinical measure: *r*, *P*)	AD (Clinical measure: *r*, *P*)	RD (Clinical measure: *r*, *P*)
AN > CN	L Fornix (crus)	%_YBC_R: +0.826, 0.043 %_QOL: −0.904, 0.013	–	YBC_R_12: −0.884, 0.02 %_YBC_R: −0.917, 0.010
	R Fornix (crus)	–	–	–
	L PTR	–	–	–
	R PTR	–	–	–
	L CC Splenium	–	–	–
	R CC Splenium	–	–	–
CN > AN	L ALIC	YBC_P_00: −0.812, 0.05	–	NS
	R ALIC	HAMD_12: +0.975, 0.001	HAMD_12: +0.831, 0.041	HAMD_12: −0.894, 0.016
	L Ant Cingulum	–	–	–
	R Ant Cingulum	NS	HAMD_00: +0.882, 0.02 BDI_00: +0.855, 0.03 YBC_R_00: +0.956, 0.003 QOL_00: −0.818, 0.047 %_QOL: +0.865, 0.026	–
	L IFO	HAMD_00: +0.830, 0.041 BDI_00: +0.910, 0.012 BAI_00: +0.855, 0.03 BAI_12: +0.891, 0.017 YBOCS_00: +0.835, 0.039 YBOCS_12: +0.821, 0.045 YBC_P_12: +0.906, 0.013 %_YBC_P: +0.935, 0.006	–	BAI_12: −0.952, 0.003 YBOCS_12: −0.807, 0.052 YBC_P_12: −0.918, 0.01 %_YBC_P: −0.847, 0.033
	R IFO	–	–	%_BAI: −0.847, 0.033
AN ∩ CN	L Post Cingulum	–	–	–
	R Post Cingulum	–	–	–
	CC Genu	–	–	–

Beck Anxiety Inventory (BAI), Beck Depression Inventory (BDI), Hamilton Depression Rating Scale (HAMD), Not significant (NS), Quality of life scale (QOL), Yale-Brown Obsessive Compulsive Scale (YBOCS), Yale-Brown-Cornell Eating Disorder Scale in women (YBC-EDS, which contains subscales for assessing ritualistic behaviours, YBC_R, and thought preoccupations related to food, YBC_P), - (Did not perform correlation given no between-group dMRI differences).
Significant ROI dMRI metrics (Fig. 3) were correlated to clinical affect-related scores (i.e. HAMD, BDI, BAI, QOL, YBOCS, YBC ritualistic/preoccupations subscales) at 12 months postsurgical time (_12), and for the percent change between pre- and post-surgery (%), using Pearson partial correlations. Brain volume and BMI scores at the time of surgery were included as control variables.

PET studies have shown bilateral, left-side dominant, reductions in parieto-occipital baseline activity in anorexia nervosa [40] which is increased following 6 months of SCC DBS [15]. Increased co-activation of the left superior parietal cortex with somatosensory and visuospatial resting state networks has also been noted, and may be related to abnormal self-body-emotional processing in anorexia nervosa [39]. Individual inspection of the MTT models revealed bilateral parieto-occipital connectivity across anorexia nervosa subjects (Table 2), although group findings show a left-side dominance. The inferior fronto-occipital fasciculus (IFO) is the longest associative bundle in the human brain [41], and decreased FA in the left IFO (Fig. 3B), and increased RD in bilateral IFO (Fig. 3D) are consistent with abnormal body perceptions and fronto-occipito-parietal functionality in anorexia nervosa [42,43]. Similar to others [44], our findings appear largely left-lateralized although increased right IFO RD also supports right parietal involvement [43,45].

The decrease in thalamic connectivity is consistent with this region as a multimodal integrator and the dysregulation of multiple brain processes in anorexia nervosa [46]. Functional imaging studies of baseline activity have identified both increases [8] and decreases [47] in thalamic activity in anorexia nervosa, and poorer behavioral flexibility is tied to lower thalamic activation along with increased frontoparietal network activity [38]. Discrepancies may be related to clinical differences in patient groups and limitations in studying thalamic nuclei, as suggested in animal models of anorexia nervosa [48,49]. Bilateral disruptions in the ALIC adjacent to the thalami – involving decreased FA and AD, and increased RD – are consistent with another dMRI study showing reduced mediodorsal thalamic FA in anorexia nervosa [50].

Affective circuitry dysfunction in anorexia nervosa

These results are in line with anorexia nervosa as a disorder involving affective circuit dysfunction [6,47]. The ventromedial prefrontal cortex, including the SCC, has recently been described as an integrative hub involved in the generation of affective meaning [51], integrating and contextualizing multimodal sensory and affective information. Recent studies have supported this role using both aversive [52,53] and appetitive [54] stimuli in humans. The SCC may be more involved in aversive, over appetitive, processing in this regard [55–57], and altered aversion-related sensorimotor and limbic area activity in anorexia nervosa is related to enhanced aversive behaviors, such as rumination and increased sensitivity to criticism and failure [58]. These findings raise the question of whether altered medial prefrontal circuits in anorexia nervosa are responsible for the misattribution of affective information to salient stimuli, such as food (often reported as disgusting in anorexia nervosa) [10] or body image (often reported as unpleasant and/or highly distorted) [39].

Using an exploratory approach, the main relationships between clinical affective measures and dMRI were noted for the left fornix crus, IFO and right ALIC. Greater improvements in self-reported quality-of-life (QOL) and aversive food-related behaviors were associated with lower pre-DBS left forniceal crus FA, suggesting that those who benefitted most from DBS originally had greater white matter disturbances in this area (Table 3). While both hippocampal and hypothalamic terminal regions of the fornix are strongly associated with food- and emotion-related behaviors [59], forniceal function is also related to improved cognitive and emotional processing in neuropsychiatric disorders such as

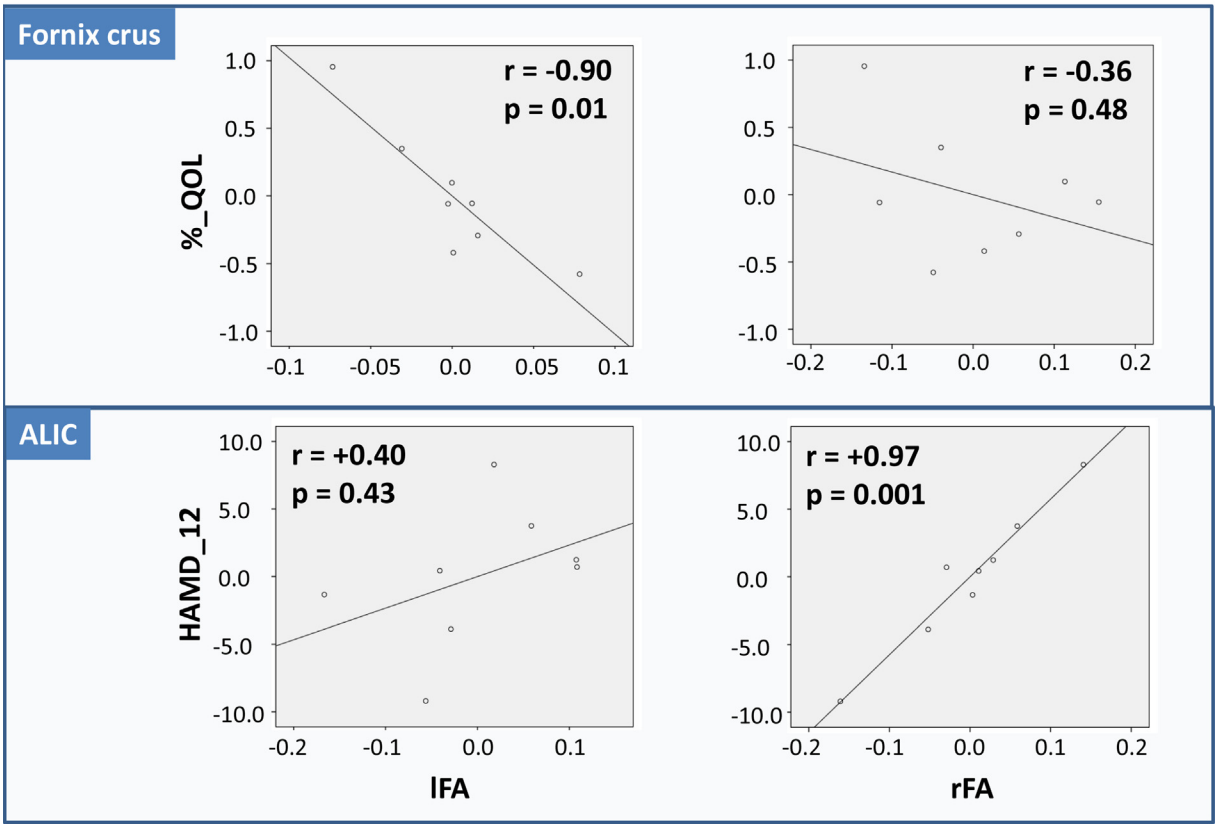

Figure 4. Partial correlations between fornix and ALIC ROIs and affect-related clinical measures. Selected Pearson partial correlations (controlling for brain volume and BMI scores at the time of surgery) highlighting that lower pre-surgical left forniceal FA values are predictive of greater increases in quality-of-life (QOL) percent score changes (taken before, and 12 months following, surgery; top left panel); while higher pre-surgical right ALIC FA values are positively correlated to depression scores at 12 months following surgery (lower right panel). These relationships do not hold for the contralateral sides of the brain. Anterior limb of the internal capsule (ALIC), l/r FA (left/right fornix crus), Hamilton depression score at 12 months post-surgery (HAMD_12), Pearson's partial correlation (r), *p*-value (*p*), Quality-of-Life score percent change from presurgery to 12 months post-surgery (%_QOL).

Alzheimer's or addiction [60,61]. Greater R ALIC and L IFO disturbances in anorexia nervosa patients were correlated with post-DBS improvements in depressive symptoms, or anxiety and eating-related symptoms, respectively (Table 3). The ALIC, and nearby medial forebrain bundle, are well-tied to reward-related processing and the mediation of depressive symptoms [62–64], whereas alterations in IFO connectivity are consistent with findings from other patient groups such as those with generalized anxiety, obsessive compulsive, and body dysmorphic disorders [65–67]. These relationships are unlikely due to general correlations with brain volume or BMI, as similar correlations were not present on the contralateral side (Fig. 4). As these exploratory clinical findings are based on few subjects filling out many questionnaires, we did not correct for multiple comparisons (e.g. increasing the likelihood of type I errors). Future studies should consider using these findings to generate *a priori* hypotheses regarding potential relationships between specific tracts and clinical outcomes.

Implications for using dMRI and DBS in anorexia nervosa

Disruptions in forniceal white matter is a consistent finding in anorexia nervosa studies [42,44,68] while changes in the IFO and ALIC are not well understood. These tracts are particularly important in the interconnection of cortical (e.g. prefrontal and insular cortices) and subcortical (e.g. ventral striatum) affective structures implicated in the effects of DBS for psychiatric illness [69]. Studies

Table 4
Summarized clinical outcomes by subject from pre-surgery to post-surgery (% score changes).

	HAMD (%)	BDI (%)	BAI (%)	YBOCS (%)	YBC_P (%)	YBC_R (%)	QOL (%)	BMI (12-base) (%)	BMI (12-0) (%)
A01	−35[a]	−21[a]	−16[a]	−28[a]	0[b]	−30[a]	70[a]	54[a]	7[a]
A02	−76[a]	−29[a]	−17[a]	−36[a]	0[b]	−26[a]	−2[b]	1[b]	−12[d]
A03	−67[a]	−28[a]	−8[b]	−65[a]	−43[a]	−37[a]	−13[d]	18[a]	14[a]
A04	23[d]	−16[a]	−11[a]	−50[c]	−13[a]	−9[a]	8[b]	−1[b]	−27[d]
A05	−86[a]	−100[a]	−76[a]	−71[a]	−46[a]	−59[a]	179[a]	31[a]	17[a]
A06	−50[c]	−50[c]	−100[a]	−64[a]	−55[a]	−52[a]	1[b]	41[a]	39[a]
A07	−80[a]	−82[a]	−72[a]	−54[a]	−35[a]	−61[a]	82[a]	31[a]	25[a]
A08	−70[a]	39[d]	−48[a]	−14[a]	−15[a]	−22[a]	−34[d]	5[b]	−7[d]

[a] Clinical improvement.
[b] No change.
[c] Not relevant (i.e. subject's score was subclinical).
[d] Clinical worsening.

in major depressive disorder – for which SCC DBS has been shown effective – revealed that lower forniceal FA values are associated with failure to achieve remission [70,71]. Although some studies show unaltered forniceal white matter in depression [72], future forniceal subregional analysis may help explain these discrepancies [73]. Although the mechanisms through which DBS exerts its impact are complex and incompletely understood [74], growing evidence supports a greater influence on diffuse white matter tracts, compared to gray matter, suggesting that methods focused on improving tract visualization, such as tractography, will be of great importance in DBS target planning in future [75].

Together, these results show that poorer pre-DBS dMRI metrics (i.e. lower FA/AD or higher RD values) in affective circuitry are associated with better post-surgical affective outcomes. Specifically, they support the notion that poorer metrics in the left fornix crus, IFO, and right ALIC are related to better affective clinical outcomes following DBS, and that the positive effects of DBS in some patients may be speculatively related to improvements in these microstructural abnormalities. If these results are confirmed, structural connectivity analyses may be used at the individual level to help tailor appropriate treatment strategies for those with anorexia nervosa.

The present approach is also relevant for the assessment of other potential targets for use in treatment-resistant anorexia nervosa, and the findings here are consistent with the hypothesis, considered previously by our group, that anorexia nervosa is intimately related to wide-spread alterations in limbic circuitry [6]. Although the SCC is a hub region with high connectivity to most limbic structures, there are also other anatomical candidates in this regard. The nucleus accumbens is one such target, particularly its associated medial forebrain white matter bundle which connects the brainstem nuclei, cerebellum, and midbrain to the basal ganglia (including the accumbens) and prefrontal cortex (including the subgenual cingulate) [76]. Many targets used in treatment-refractory major depressive disorder, such as the SCC, anterior limb of the internal capsule, and nucleus accumbens, are all connected by fibers of the medial forebrain bundle [62,63]. Also, as DBS does not result in clinical improvements for all people with major depressive disorder [62,77], it will be important going forward to precisely determine which anorexia nervosa patients respond best to DBS. Regardless, it appears that dMRI techniques, including mutli-tensor tractography, will be key in determining the best targeting for such effects and may eventually become part of standard pre-surgical planning [75,78,79].

Limitations & future directions

Limitations include a low number of subjects with heterogenous anorexia nervosa symptoms, co-morbidities, medication use, and comparisons of healthy against chronically nutrient deficient people [80]. We used total brain volumes and BMI values at the time of surgery as covariates in our analyses to partially control for such effects. Although medication use (e.g. SSRIs) alters the brain, some studies have reported no differences between anorexia nervosa patients taking or not taking SSRIs [81]. Future technical improvements could include the acquisition of thinner slices (below the 3 mm slices acquired here) and the use of a 32 or 64 channel head coil if possible. Additionally, although regionally-selective dMRI metrics are correlated to some post-surgical improvements, we are currently unable to determine if these improvements are related to corresponding changes in white matter structure because dMRI cannot be performed post-DBS due to the indwelling electrode.

Exploratory findings between the clinical effects of deep brain stimulation and dMRI-based measures are promising, but did not reveal a consistent pattern between structural abnormalities and behaviour. For instance, regional differences between patients and controls could relate to pre- or post-surgical affective psychometrics and it is not clear if the pre-surgical dMRI values are predicting affective changes or are correlated through other variables – such as generally poorer white matter metrics being associated with a greater chance of clinical improvement. Although unsurprising, given the highly complex and heterogenous nature of the disorder, future analyses will need to disentangle these results by including psychometric data from healthy controls and those with differences in AN symptom severity. Future studies should also consider investigating whether gray matter differences exist in white matter regions identified here – as this could not be explored in the present study due to technical limitations (see Supplementary Methods section).

Finally, the present study included one left-handed patient without a corresponding left-handed healthy control. Although there were no obvious differences in the individual MTT map, or obvious lateral differences in the dMRI values, of the left-handed subject, this should be considered in future studies given many reports of differences in brain laterality in this patient group. For example, how the current results are tied to findings of reduced serotonin 2A receptor binding in the left subgenual and parietal, and right occipital, cortices [19], or asymmetrical functional differences in the temporal cortex, amygdala and insula during the resting state [82], is unknown. It will, for instance, be interesting to see if some of these anorexia-associated asymmetries in structure and function are directly related to those seen in response to affective stimuli [55].

These considerable limitations underscore the need for follow-up study, both in AN patients undergoing DBS as well as those undergoing non-DBS treatments for this disorder. Moreover, the future application of dMRI before and after such treatments will help to clarify the relationship, if any, of white matter alterations within the SCC and its associated connections to clinical outcomes. Nonetheless, the present study points to avenues of future investigation and helps to generate clear hypotheses around regional white matter alterations and their potential clinical relevance.

Conclusion

The present study revealed differences between SCC connectivity in anorexia nervosa compared to healthy controls. Differences in dMRI metrics along affect-related tracts may point to widespread structural abnormalities in this disorder. While the group analysis suggested most differences in anorexia nervosa were on the left side, ROI analysis revealed bilateral changes. Abnormalities in tracts connecting the medial prefrontal cortex to other key cortical (e.g. parietal, occipital, insular) and subcortical (e.g. striatal, thalamic) regions identified in anorexia nervosa pathology are largely consistent with a central role for dysfunctional affective processing and broad clinical changes (e.g. alterations in the processing of affective stimuli, self-perception, and interoception).

Appendix. Supplementary data

Supplementary data related to this article can be found at http://dx.doi.org/10.1016/j.brs.2015.03.005.

References

[1] Sullivan P. Mortality in anorexia nervosa. Am J Psychiatry 1995;152:1073–4.
[2] Arcelus J, Mitchell AJ, Wales J. Mortality rates in patients with anorexia nervosa and other eating disorders. A meta-analysis of 36 studies. Arch Gen Psychiatry 2013;68:724–31.
[3] Fitzpatrick KK, Lock J. Anorexia nervosa. BMJ Clin Evid 2011;2011:1–36.

[4] Flament MF, Bissada H, Spettigue W. Evidence-based pharmacotherapy of eating disorders. Int J Neuropsychopharmacol 2012;15:189–207.
[5] Attia E. Anorexia nervosa: current status and future directions. Annu Rev Med 2010;61:425–35.
[6] Lipsman N, Woodside DB, Lozano AM. Neurocircuitry of limbic dysfunction in anorexia nervosa. Cortex 2014;62:109–18.
[7] Delvenne V, Lotstra F, Goldman S, et al. Brain hypometabolism of glucose in anorexia nervosa: a PET scan study. Biol Psychiatry 1995;37:161–9.
[8] Takano A, Shiga T, Kitagawa N, et al. Abnormal neuronal network in anorexia nervosa studied with I-123-IMP SPECT. Psychiatry Res 2001;107:45–50.
[9] Ellison Z, Foong J, Howard R, Bullmore E. Functional anatomy of calorie fear in anorexia nervosa. Lancet 1998;352:1998.
[10] Uher R, Brammer MJ, Murphy T, et al. Recovery and chronicity in anorexia nervosa. Biol Psychiatry 2003;54:934–42.
[11] Fladung A-K, Schulze UM, Schöll F, Bauer K, Grön G. Role of the ventral striatum in developing anorexia nervosa. Transl Psychiatry 2013;3:e315.
[12] Miyake Y, Okamoto Y, Onoda K, et al. Brain activation during the perception of distorted body images in eating disorders. Psychiatry Res 2010;181:183–92.
[13] Wagner A, Aizenstein H, Venkatraman V, et al. Altered reward processing in women recovered from anorexia nervosa. Am J Psychiatry 2007;164:1842–9.
[14] Wagner A, Aizenstein H, Mazurkewicz L, et al. Altered insula response to taste stimuli in individuals recovered from restricting-type anorexia nervosa. Neuropsychopharmacology 2008;33:513–23.
[15] Lipsman N, Woodside DB, Giacobbe P, et al. Subcallosal cingulate deep brain stimulation for treatment-refractory anorexia nervosa: a phase 1 pilot trial. Lancet 2013;381:1361–70.
[16] Lipsman N, Woodside DB, Giacobbe P, Lozano AM. Neurosurgical treatment of anorexia nervosa: review of the literature from leucotomy to deep brain stimulation. Eur Eat Disord Rev 2013;21:428–35.
[17] Suetens K, Nuttin B, Gabriëls L, Van Laere K. Differences in metabolic network modulation between capsulotomy and deep-brain stimulation for refractory obsessive-compulsive disorder. J Nucl Med 2014;55:951–9.
[18] Cooney RE, Joormann J, Eugène F, Dennis EL, Gotlib IH. Neural correlates of rumination in depression. Cogn Affect Behav Neurosci 2010;10:470–8.
[19] Bailer UF, Price JC, Meltzer CC, et al. Altered 5-HT(2A) receptor binding after recovery from bulimia-type anorexia nervosa: relationships to harm avoidance and drive for thinness. Neuropsychopharmacology 2004;29:1143–55.
[20] Bailer U, Frank G. Altered brain serotonin 5-HT1A receptor binding after recovery from anorexia nervosa measured by positron emission tomography and WAY-100635. Arch Gen Psychiatry 2005;62:1032–41.
[21] Johansen-Berg H, Gutman DA, Katz E, et al. Anatomical connectivity of the subgenual cingulate region targeted with deep brain stimulation for treatment-resistant depression. Cereb Cortex 2008;18:1374–83.
[22] Seminowicz DA, Mayberg HS, McIntosh AR, et al. Limbic-frontal circuitry in major depression: a path modeling metanalysis. Neuroimage 2004;22:409–18.
[23] Wang G, Erpelding N, Davis KD. Sex differences in connectivity of the subgenual anterior cingulate cortex. Pain 2014;155:755–63.
[24] Khalsa S, Mayhew SD, Chechlacz M, Bagary M, Bagshaw AP. The structural and functional connectivity of the posterior cingulate cortex: comparison between deterministic and probabilistic tractography for the investigation of structure-function relationships. Neuroimage 2013. 102 Pt 1:118–127.
[25] Descoteaux M, Deriche R, Knösche TR, Anwander A. Deterministic and probabilistic tractography based on complex fibre orientation distributions. IEEE Trans Med Imaging 2009;28:269–86.
[26] Qazi AA, Radmanesh A, O'Donnell L, et al. Resolving crossings in the corticospinal tract by two-tensor streamline tractography: method and clinical assessment using fMRI. Neuroimage 2009;47(Suppl. 2):T98–106.
[27] Smith SM, Jenkinson M, Woolrich MW, et al. Advances in functional and structural MR image analysis and implementation as FSL. Neuroimage 2004;23(Suppl. 1):S208–19.
[28] Pieper S, Halle M, Kikinis R. 3D Slicer. Proc 1st IEEE Int Symp Biomed Imaging 2004;1:632–5.
[29] Leemans A, Jones DK. The B-matrix must be rotated when correcting for subject motion in DTI data. Magn Reson Med 2009;61:1336–49. http://dx.doi.org/10.1002/mrm.21890.
[30] Gutman DA, Holtzheimer PE, Behrens TEJ, Johansen-Berg H, Mayberg HS. A tractography analysis of two deep brain stimulation white matter targets for depression. Biol Psychiatry 2009;65:276–82.
[31] Hamilton M. A rating scale for depression. J Neurol Neurosurg Psychiatry 1960;23:56–62.
[32] Beck A, Steer R, Ball R, Ranieri W. Comparison of Beck depression 1 in psychiatric inventories -1A and – outpatients. J Pers Assess 1996;67:588–97.
[33] Beck AT, Epstein N, Brown G, Steer RA. An inventory for measuring clinical anxiety: psychometric properties. J Consult Clin Psychol 1988;56:893–7.
[34] Goodman W. The Yale-Brown obsessive compulsive scale: I. Development, use, and reliability. Arch Gen Psychiatry 1989;46:1006–11.
[35] Mazure C, Halmi K, Sunday S. The Yale-Brown-Cornell eating disorder scale: development, use, reliability and validity. J Psychiatr Res 1994;3956:425–45.
[36] Flanagan J. A research approach to improving our quality of life. Am Psychol 1978;33:138–47.
[37] Riva-Posse P, Sueng Choi K, Holtzheimer PE, et al. Defining critical white matter pathways mediating successful subcallosal cingulate deep brain stimulation for treatment-resistant depression. Biol Psychiatry 2014;76:963–9.
[38] Zastrow A, Kaiser S. Neural correlates of impaired cognitive-behavioral flexibility in anorexia nervosa. Am J Psychiatry 2009;166:608–16.
[39] Favaro A, Santonastaso P, Manara R, et al. Disruption of visuospatial and somatosensory functional connectivity in anorexia nervosa. Biol Psychiatry 2012;72:864–70.
[40] Zhang H, Zuo C, Sun B. Metabolic imaging of deep brain stimulation in anorexia nervosa. Soc Nucl Med 2012;38:943–8.
[41] Caverzasi E, Papinutto N, Amirbekian B, Berger MS, Henry RG. Q-Ball of inferior fronto-occipital fasciculus and beyond. PLoS One 2014;9:e100274.
[42] Kazlouski D, Rollin MDH, Tregellas J, et al. Altered fimbria-fornix white matter integrity in anorexia nervosa predicts harm avoidance. Psychiatry Res 2011;192:109–16.
[43] Castellini G, Polito C, Bolognesi E, et al. Looking at my body. Similarities and differences between anorexia nervosa patients and controls in body image visual processing. Eur Psychiatry 2013;28:427–35.
[44] Via E, Zalesky A, Sánchez I. Disruption of brain white matter microstructure in women with anorexia nervosa. J Psychiatry Neurosci 2014;39:130–5.
[45] Nico D, Daprati E, Nighoghossian N, Carrier E, Duhamel J-R, Sirigu A. The role of the right parietal lobe in anorexia nervosa. Psychol Med 2010;40:1531–9.
[46] Metzger C. Functional mapping of thalamic nuclei and their integration into cortico-striatal-thalamo-cortical loops via ultra-high resolution imaging—from animal anatomy. Front Neurosci 2013;7:1–14.
[47] Chowdhury U, Gordon I, Lask B, Watkins B, Watt H, Christie D. Early-onset anorexia nervosa: is there evidence of limbic system imbalance? Int J Eat Disord 2003;33:388–96.
[48] Barbarich-Marsteller N, Marsteller D. MicroPET imaging in an animal model of anorexia nervosa. Synapse 2005;90:85–90.
[49] Luyten L, Welkenhuysen M, van Kuyck K, et al. The effects of electrical stimulation or an electrolytic lesion in the mediodorsal thalamus of the rat on survival, body weight, food intake and running activity in the activity-based anorexia model. Brain Res Bull 2009;79:116–22.
[50] Frieling H, Fischer J, Wilhelm J, et al. Microstructural abnormalities of the posterior thalamic radiation and the mediodorsal thalamic nuclei in females with anorexia nervosa – a voxel based diffusion tensor imaging (DTI) study. J Psychiatr Res 2012;46:1237–42.
[51] Roy M, Shohamy D, Wager TD. Ventromedial prefrontal-subcortical systems and the generation of affective meaning. Trends Cogn Sci 2012;16:147–56.
[52] Hayes DJ, Duncan NW, Wiebking C, et al. GABAA receptors predict aversion-related brain responses: an fMRI-PET investigation in healthy humans. Neuropsychopharmacology 2013;38:1438–50.
[53] Lipsman N, Kaping D, Westendorff S, Sankar T, Lozano AM, Womelsdorf T. Beta coherence within human ventromedial prefrontal cortex precedes affective value choices. Neuroimage 2014;85(Pt 2):769–78.
[54] Kirk U, Gu X, Harvey AH, Fonagy P, Montague PR. Mindfulness training modulates value signals in ventromedial prefrontal cortex through input from insular cortex. Neuroimage 2014;100:254–62.
[55] Hayes DJ, Duncan N, Xu J, Northoff G. A comparison of neural responses to appetitive and aversive stimuli in humans and other mammals. Neurosci Biobehav Rev 2014;45:350–68.
[56] Laxton AW, Neimat JS, Davis KD, et al. Neuronal coding of implicit emotion categories in the subcallosal cortex in patients with depression. Biol Psychiatry 2013;74:714–9.
[57] Amemori K, Graybiel AM. Localized microstimulation of primate pregenual cingulate cortex induces negative decision-making. Nat Neurosci 2012;15:776–85.
[58] Bischoff-Grethe A, McCurdy D, Grenesko-Stevens E, et al. Altered brain response to reward and punishment in adolescents with anorexia nervosa. Psychiatry Res 2013;214:331–40.
[59] Berthoud H-R, Morrison C. The brain, appetite, and obesity. Annu Rev Psychol 2008;59:55–92.
[60] Smith GS, Laxton AW, Tang-Wai DF, et al. Increased cerebral metabolism after 1 year of deep brain stimulation in Alzheimer disease. Arch Neurol 2012;69:1141–8.
[61] Schulte T. Neurocircuitry of emotion and cognition in alcoholism: contributions from white matter fiber tractography. Dialogues Clin Neurosci 2010;12:554–60.
[62] Schlaepfer TE, Bewernick BH, Kayser S, Hurlemann R, Coenen VA. Deep brain stimulation of the human reward system for major depression – rationale, outcomes and outlook. Neuropsychopharmacology 2014;39:1303–14.
[63] Coenen VA, Honey CR, Hurwitz T, et al. Medial forebrain bundle stimulation as a pathophysiological mechanism for hypomania in subthalamic nucleus deep brain stimulation for Parkinson's disease. Neurosurgery 2009;64:1106–15.
[64] Blood AJ, Iosifescu DV, Makris N, et al. Microstructural abnormalities in subcortical reward circuitry of subjects with major depressive disorder. PLoS One 2010;5:e13945.
[65] Liao M, Yang F, Zhang Y, He Z, Su L, Li L. White matter abnormalities in adolescents with generalized anxiety disorder: a diffusion tensor imaging study. BMC Psychiatry 2014;14:41.
[66] Li F, Huang X, Tang W, et al. Multivariate pattern analysis of DTI reveals differential white matter in individuals with obsessive-compulsive disorder. Hum Brain Mapp 2014;35:2643–51.

[67] Buchanan BG, Rossell SL, Maller JJ, Toh WL, Brennan S, Castle DJ. Brain connectivity in body dysmorphic disorder compared with controls: a diffusion tensor imaging study. Psychol Med 2013;43:2513–21.
[68] Nagahara Y, Nakamae T, Nishizawa S, et al. A tract-based spatial statistics study in anorexia nervosa: abnormality in the fornix and the cerebellum. Prog Neuropsychopharmacol Biol Psychiatry 2014;51:72–7.
[69] Lehman JF, Greenberg BD, McIntyre CC, Rasmussen SA, Haber SN. Rules ventral prefrontal cortical axons use to reach their targets: implications for diffusion tensor imaging tractography and deep brain stimulation for psychiatric illness. J Neurosci 2011;31:10392–402.
[70] Hoogenboom WS, Perlis RH, Smoller JW, et al. Limbic system white matter microstructure and long-term treatment outcome in major depressive disorder: a diffusion tensor imaging study using legacy data. World J Biol Psychiatry 2014;15:122–34.
[71] Korgaonkar MS, Williams LM, Song YJ, Usherwood T, Grieve SM. Diffusion tensor imaging predictors of treatment outcomes in major depressive disorder. Br J Psychiatry 2014;205:321–8.
[72] Bracht T, Jones DK, Müller TJ, Wiest R, Walther S. Limbic White matter microstructure plasticity reflects recovery from depression. J Affect Disord 2014;170:143–9.
[73] Chen D, Strauss I, Hayes D, Davis K, Hodaie M. Age-related changes in diffusion tensor imaging metrics of fornix subregions in healthy humans. Stereotact Funct Neurosurg 2014;93:151–9.
[74] Chen XL, Xiong YY, Xu GL, Liu XF. Deep brain stimulation. Interv Neurol 2013;1:200–12.
[75] Torres CV, Manzanares R, Sola RG. Integrating diffusion tensor imaging-based tractography into deep brain stimulation surgery: a review of the literature. Stereotact Funct Neurosurg 2014;92:282–90.
[76] Coenen VA, Schlaepfer TE, Maedler B, Panksepp J. Cross-species affective functions of the medial forebrain bundle-Implications for the treatment of affective pain and depression in humans. Neurosci Biobehav Rev 2011;35:1971–81. http://dx.doi.org/10.1016/j.neubiorev.2010.12.009.
[77] Schlaepfer TE, Bewernick BH, Kayser S, Mädler B, Coenen VA. Rapid effects of deep brain stimulation for treatment-resistant major depression. Biol Psychiatry 2013;73:1204–12. http://dx.doi.org/10.1016/j.biopsych.2013.01.034.
[78] Coenen VA, Schlaepfer TE, Allert N, Mädler B. Diffusion tensor imaging and neuromodulation: DTI as key technology for deep brain stimulation. Int Rev Neurobiol 2012;107:207–34. http://dx.doi.org/10.1016/B978-0-12-404706-8.00011-5.
[79] Farquharson S, Tournier J-D, Calamante F, et al. White matter fiber tractography: why we need to move beyond DTI. J Neurosurg 2013;118:1367–77. http://dx.doi.org/10.3171/2013.2.JNS121294.
[80] Amianto F, Caroppo P, D'Agata F, et al. Brain volumetric abnormalities in patients with anorexia and bulimia nervosa: a voxel-based morphometry study. Psychiatry Res 2013;213:210–6.
[81] Brooks SJ, O'Daly OG, Uher R, et al. Differential neural responses to food images in women with bulimia versus anorexia nervosa. PLoS One 2011;6:e22259.
[82] Van Kuyck K, Gérard N, Van Laere K, et al. Towards a neurocircuitry in anorexia nervosa: evidence from functional neuroimaging studies. J Psychiatr Res 2009;43:1133–45.